Electronic Supplementary Information (ESI)

Catalytic ozonation of dichloromethane at low temperature and even room temperature on Mn-loaded catalysts

Yaxin Duan[a], Peixi Liu[a], Fawei Lin[b], Yong He[a], Yanqun Zhu[a], Zhihua Wang[a]

[a]*State Key Laboratory of Clean Energy Utilization, Zhejiang University, Hangzhou 310027, P.R. China*
[b]*School of Environmental Science and Engineering, Tianjin University, Tianjin 300072, P.R. China*

*Corresponding authors.
E-mail Address: wangzh@zju.edu.cn (ZH. Wang)

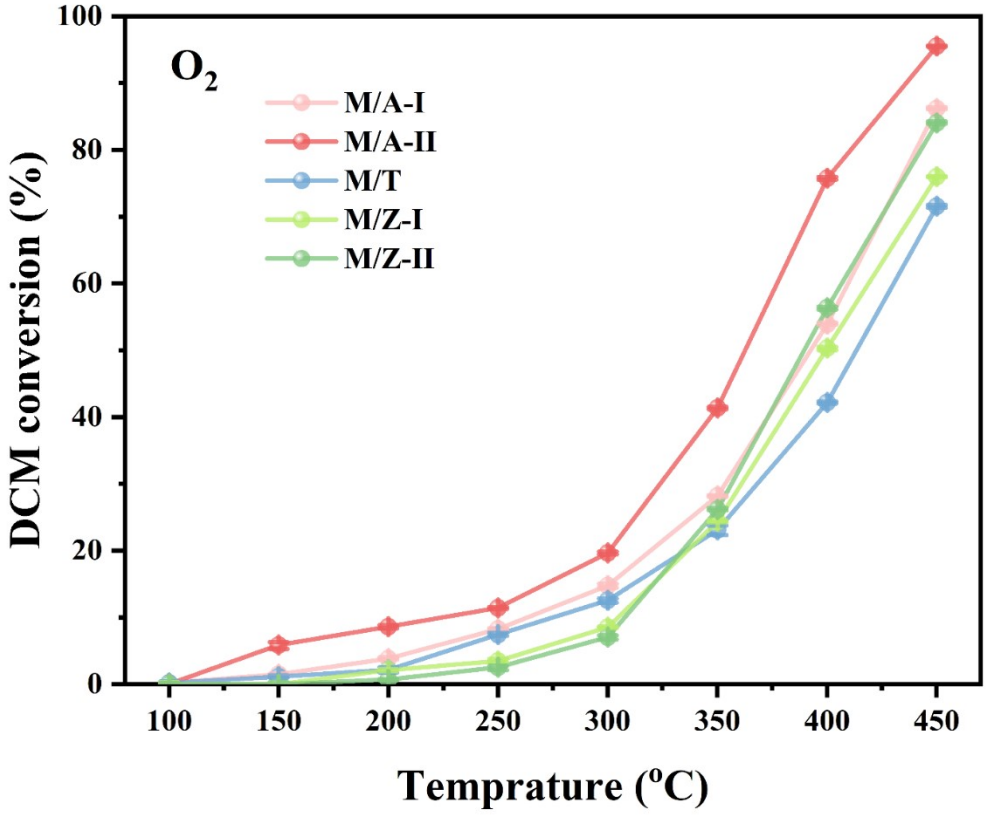

Fig. S1. DCM conversion curves at 100 ~ 450 °C of O_2 catalytic oxidation over the samples.

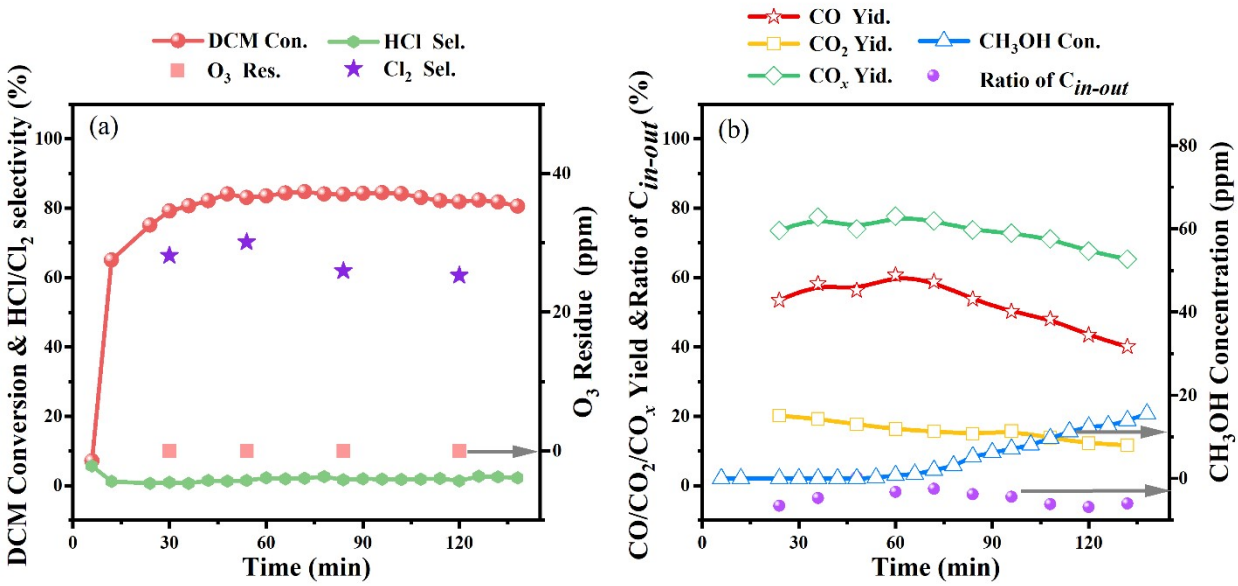

Fig. S2. Stability performance of the M/A-II with O_3/DCM=6 at 20 °C. (conditions: DCM initial concentration = 100 ppm; GHSV ≈ 30000 h^{-1}).

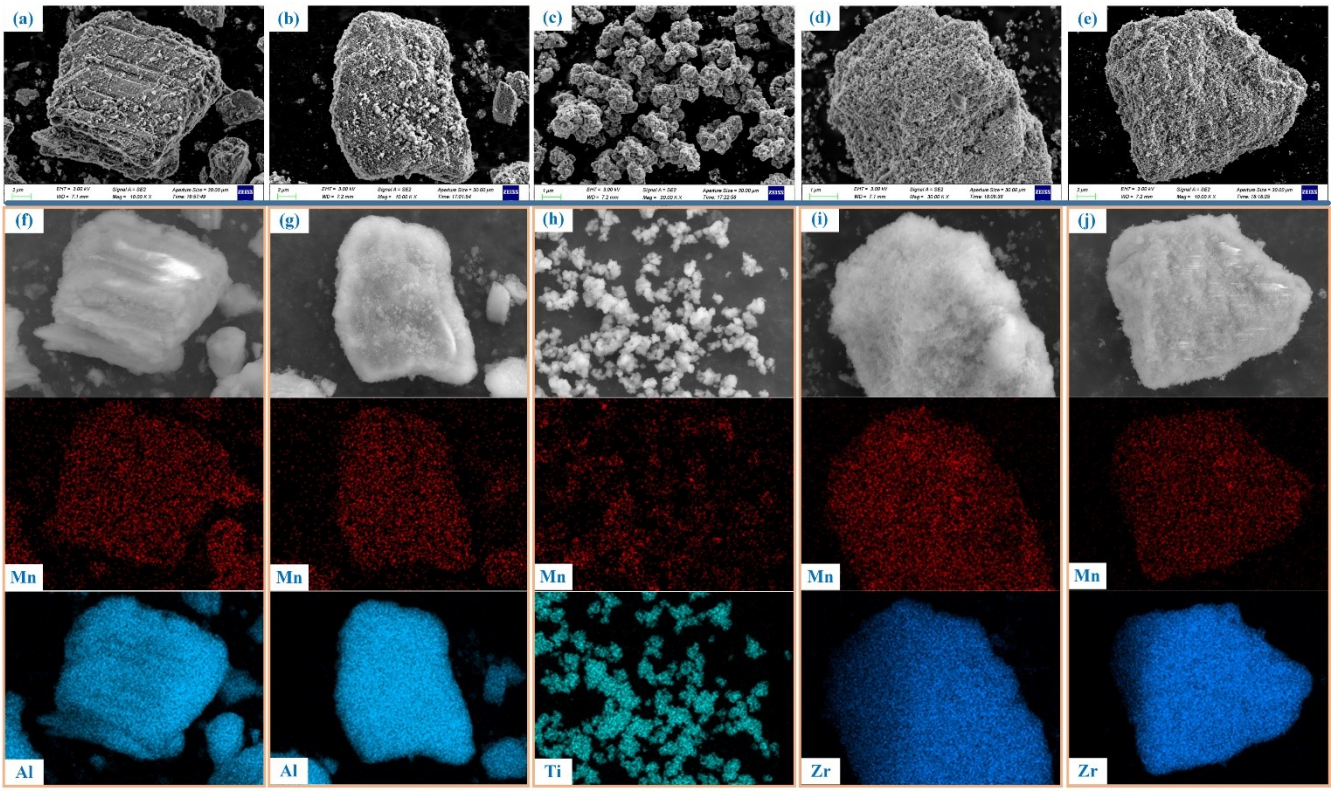

Fig. S3. (a) ~ (e) SEM and (f) ~ (j) EDS mapping images of all catalysts. (a) ~ (e) and (f) ~ (j) correspond to M/A-I, M/A-II, M/T, M/Z-I and M/Z-II in order, respectively.

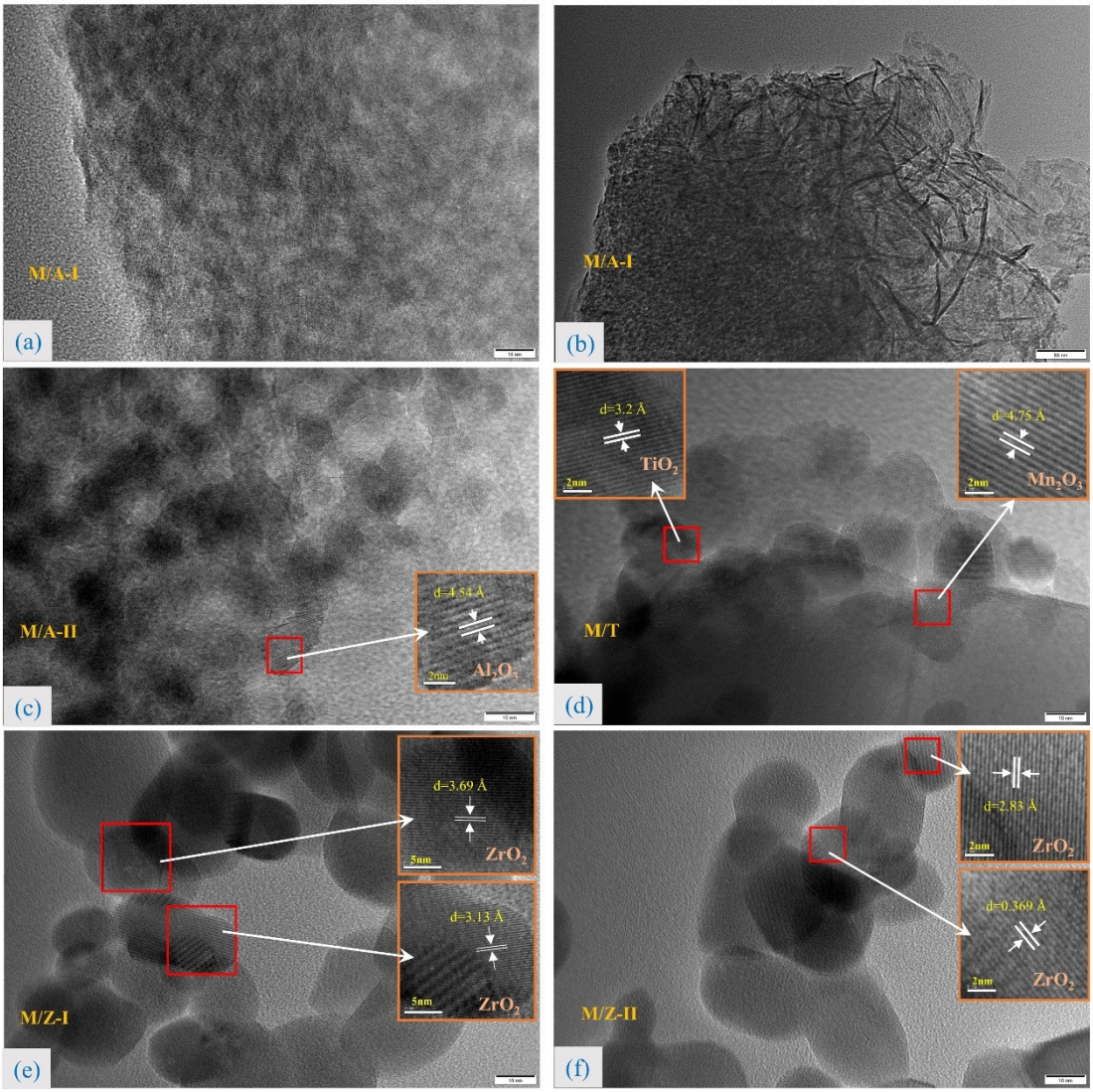

Fig. S4. TEM images of all catalysts. (a) and (b) correspond to M/A-I, and (c) ~ (f) correspond to M/A-II, M/T, M/Z-I and M/Z-II, respectively. (Due to the lack of high photographic magnification, the M/A- I data can be roughly FFT measured to a lattice spacing of 2.41 Å, which can correspond to the converted lattice spacing of PDF# 04-0877 for Al_2O_3)

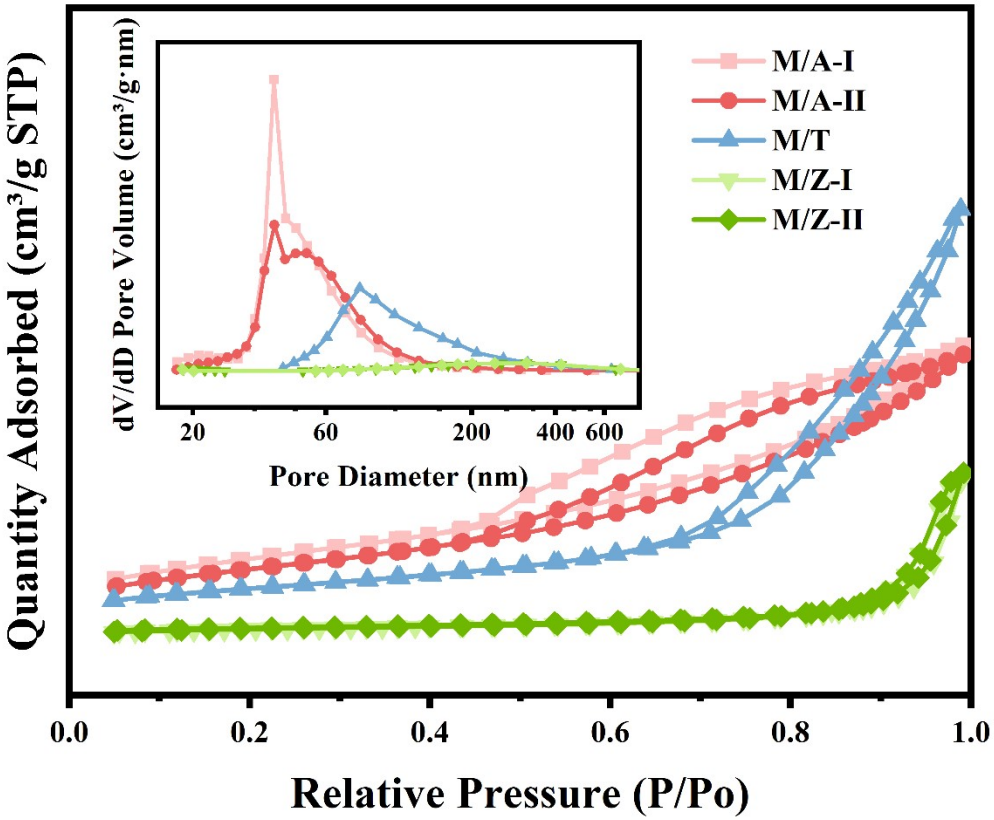

Fig. S5. N_2 adsorption and desorption isotherms and pore size distribution curves of Mn-loaded catalysts.

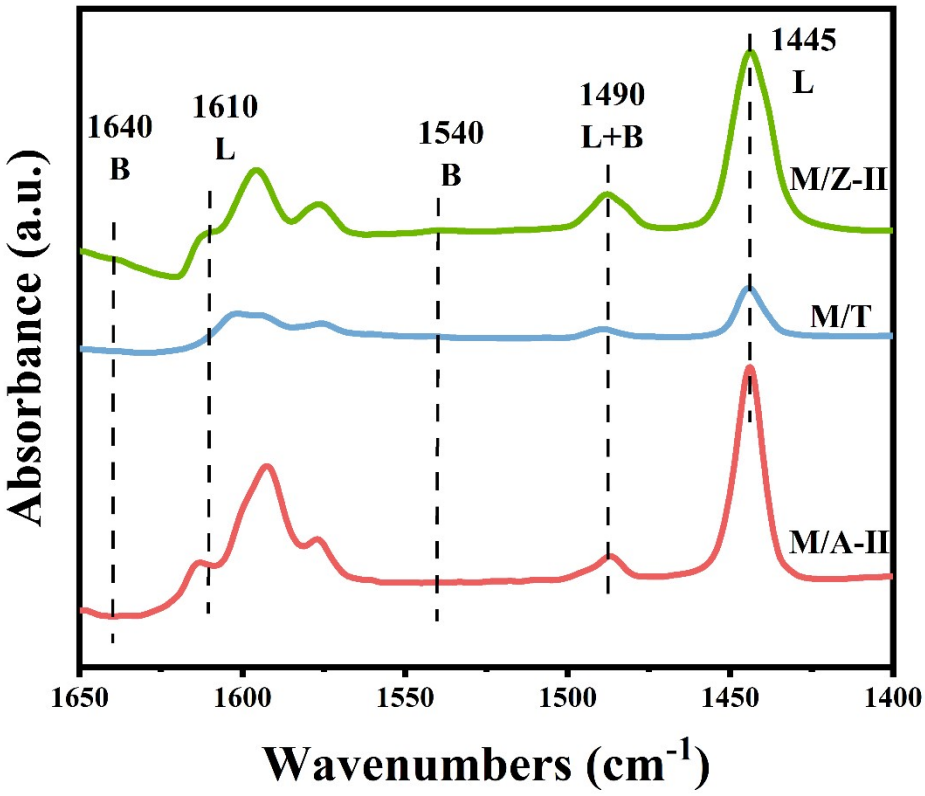

Fig. S6. Py-IR spectra of M/Z-II, M/T and M/A-II.

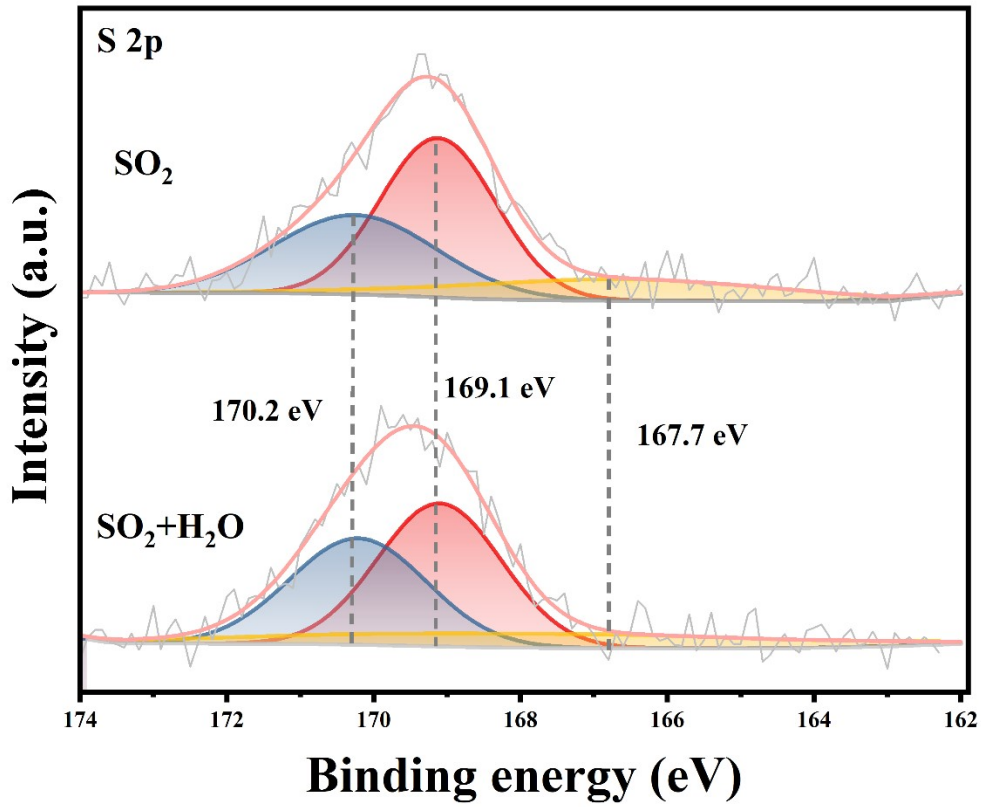

Fig. S7. XPS spectrum of S 2p after SO_2 single and both SO_2 and H_2O effect.

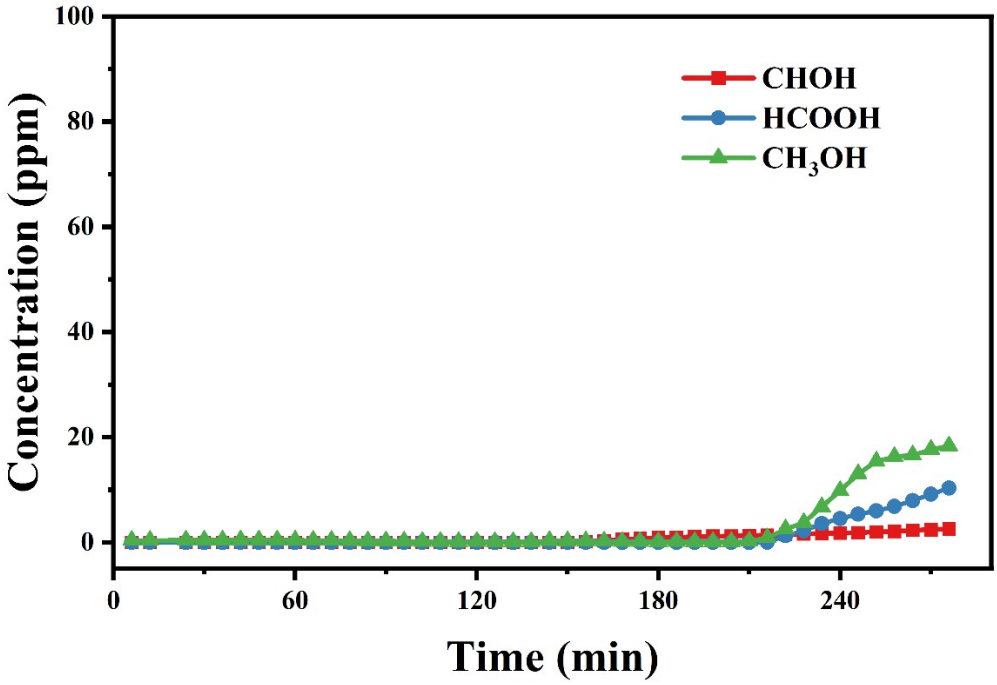

Fig. S8. Byproducts concentration of DCM ozone catalytic oxidation on M/A-II with the dynamic effects of SO_2.

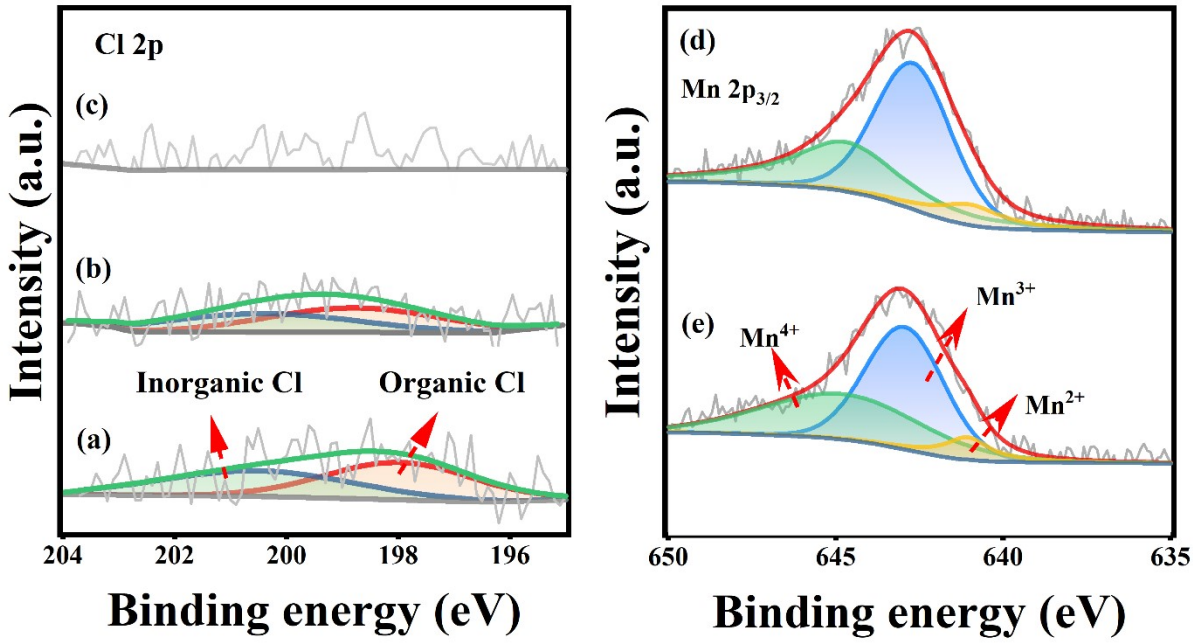

Fig. S9. XPS spectrum of Cl 2p after (a) 20 ºC stability test (b) 120 ºC stability test and (c) 120 ºC H_2O effect test; and the Mn $2p_{2/3}$ after catalytic ozonation on the M/A-II with the effects of (d) SO_2 and (e) simultaneous presence of water vapor and SO_2.

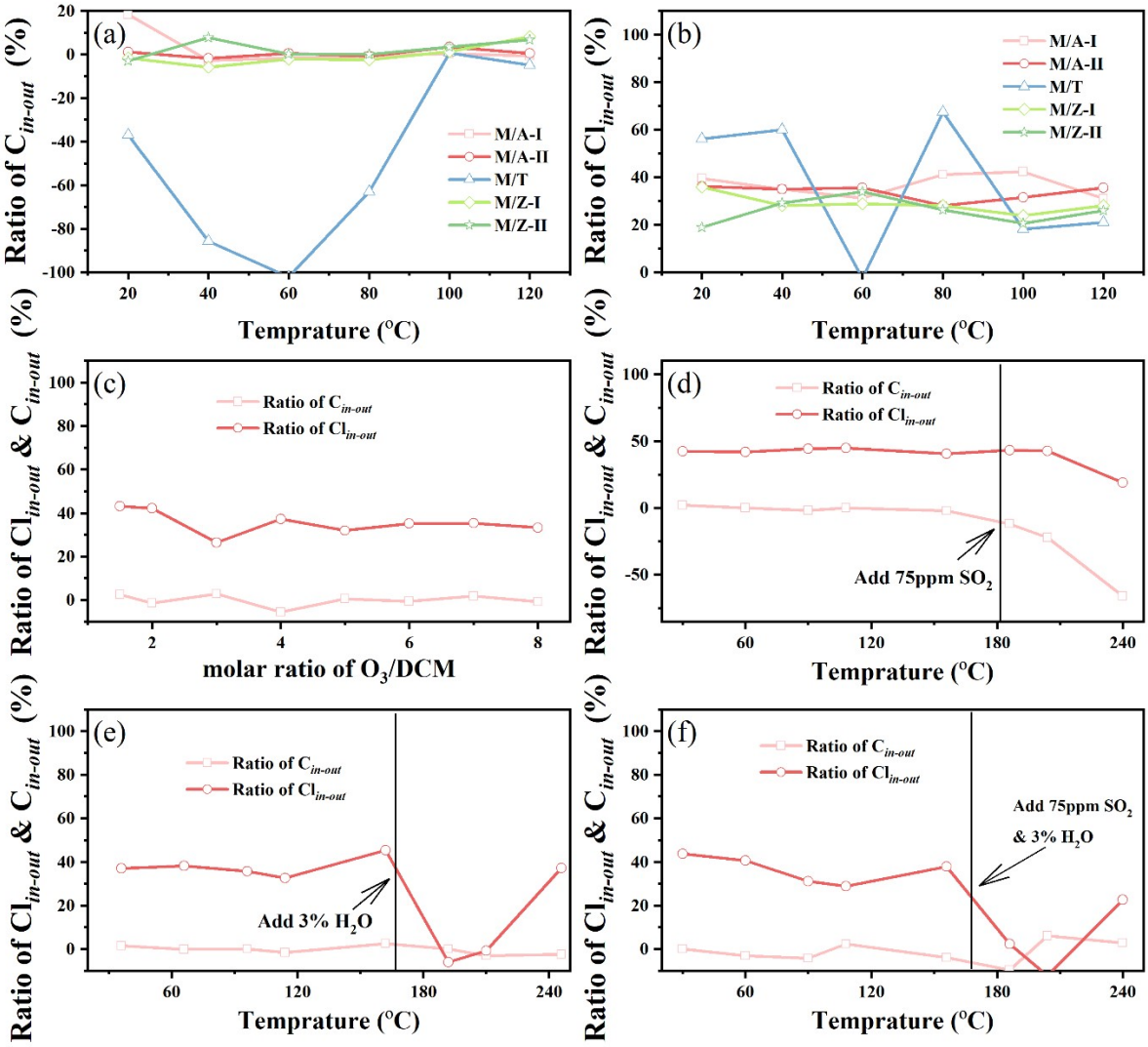

Fig. S10. Carbon/chlorine balance plots for all catalytic reactions in this study. (a) and (b) are the five catalysts carbon balance and chlorine balance from 20 ~ 120 °C reactions, respectively, corresponding to Fig. 2 (a) ~ (d) in the revised version; (c) is the reaction of changing the initial molar ratio of O_3/DCM at 120 °C on M/A-II, corresponding to Fig. 2 (e) ~ (f) in the revised version. Fig. 2 (e) ~ (f) in the revised version. (d) to (f) are the reactions at 120 °C on M/A-II when SO_2, water vapor, and both SO_2 and water vapor are introduced.

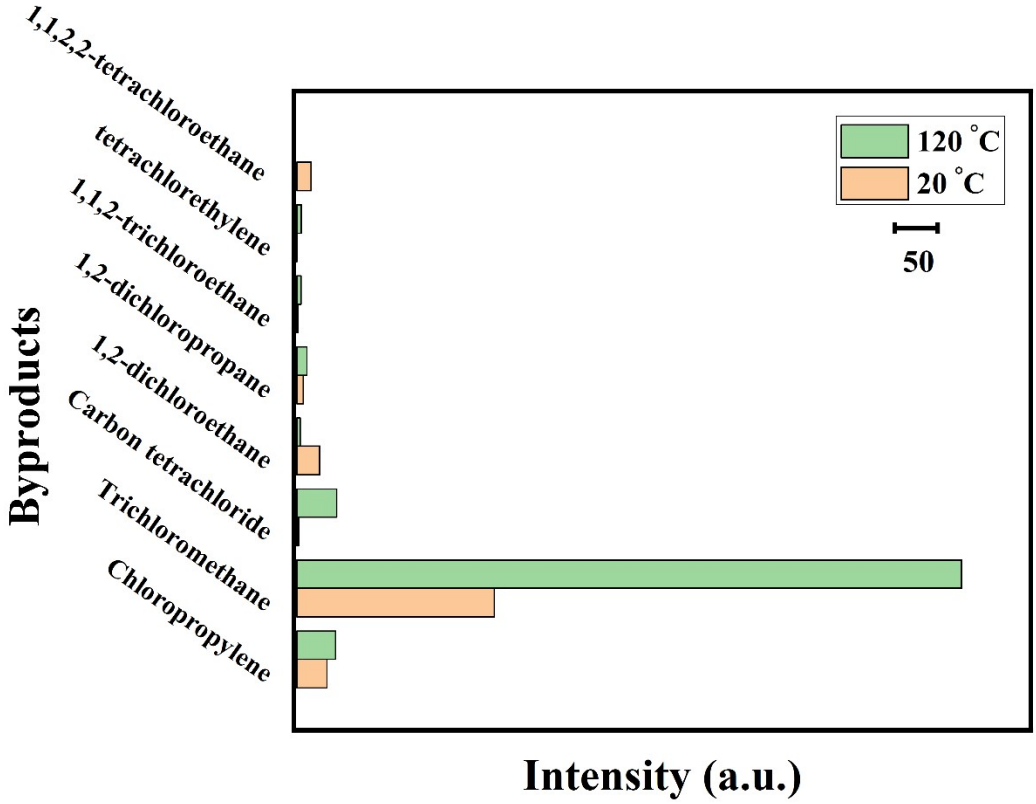

Fig. S11. By-products of catalytic ozonation of DCM at 20 °C and 120 °C on M/A-II measured by CG-MS after collection in adsorption tubes.

Table S1

Binding energy and species distribution of Mn $2p_{2/3}$ for M/A-II in different reaction environments.

Catalysts	Mn $2p_{2/3}$					
	Mn^{2+} (eV)	Mn^{3+} (eV)	Mn^{4+} (eV)	Mn^{2+}/Mn (%)	Mn^{3+}/Mn(%)	Mn^{4+}/Mn(%)
Fresh M/A-II	/	642.68	644.43	/	69.84	30.16
SO_2 M/A-II	641.00	642.69	644.71	9.87	60.03	30.09
SO_2+H_2O M/A-II	641.08	642.96	644.79	7.92	59.36	29.50

Table S2

The specific information on the by-products of the exhaust gas detected by GC-MS after adsorption tube collection.

No.	Molecular name	Molecule formula	Molecular structure
1	Chloropropylene	C_3H_5Cl	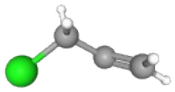
2	Trichloromethane	$CHCl_3$	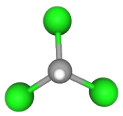
3	Carbon tetrachloride	CCl_4	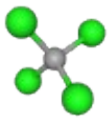
4	1,2-dichloroethane	$C_2H_4Cl_2$	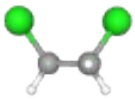
5	1,2-dichloropropane	$C_3H_6Cl_2$	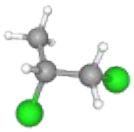
6	1,1,2-trichloroethane	$C_2H_3Cl_3$	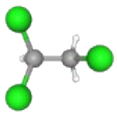
7	Tetrachlorethylene	C_2Cl_4	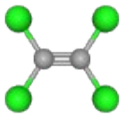
8	1,1,2,2-tetrachloroethane	$C_2H_2Cl_4$	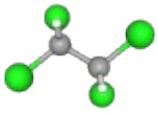

According to **Fig. S11**, that all experiments have reached the carbon balance within 10% error range. For the chlorine balance, the visible chlorine balance only reaches 60 ~ 80% in the absence of water vapor. When a high concentration of water vapor was introduced, the value of Ratio of $Cl_{in\text{-}out}$ decreased to nearly zero and the visible chlorine balance was achieved. In addition, the carbon balance deviated from normal in **Fig. S11** (a) when reacting on M/T at 20 ~ 60 °C. One reason is that M/T has poor low temperature performance and cannot oxidize DCM to CO_x, thus generating more byproducts CH_3OH which may compete with DCM. The second reason is the higher boiling point of CH_3OH, i.e., CH_3OH (64.7 °C) > DCM (39.8 °C), which could stay on the surface of M/T and affect the carbon balance. Similarly, in **Fig. S11** (d), after the poisoning of M/A-II by the erosion of high concentration of SO_2, more CH_3OH production was detected at the same time. Therefore, it could be said that the poisoned M/A-II also had difficulty in resisting the CH_3OH production and the carbon balance deviated from the normal.